Overview of Moment Tensor Analysis in New Zealand

John Ristau

1 Introduction

The determination of earthquake source parameters is of fundamental importance in seismological research. Moment tensor analysis involves fitting theoretical waveforms to observed broadband waveforms and inverting for the moment tensor elements, and allows for the calculation of focal mechanism (strike, dip, and rake), seismic moment (M_0), moment magnitude (M_w) which is calculated directly from M_0, and centroid depth of an earthquake. A comprehensive catalogue of moment tensor solutions is of great importance in seismic hazard analysis and tectonic studies. For example, seismic hazard estimates typically use M_w in earthquake forecasts and risk analysis, and moment release rates along plate boundaries are important in calculating predicted plate motions in tectonic studies. Routine regional moment tensor (RMT) analysis was implemented in New Zealand in early-2007 (Ristau 2008), and since that time more than 2000 RMT solutions have been calculated for New Zealand earthquakes with the catalogue beginning August 2003. This article will provide an overview of RMT analysis in New Zealand with specific focus on five earthquake sequences which significantly impacted New Zealand since July 2009.

2 Tectonic Setting of New Zealand

New Zealand straddles the boundary of the Pacific and Australian plates, and the active tectonics are dominated by three main features (Fig. 1). North Island seismicity ranges from shallow activity with surface ruptures to events with hypocentres

J. Ristau (✉)
GNS Science, Lower Hutt, New Zealand
e-mail: j.ristau@gns.cri.nz

S. D'Amico (ed.), *Moment Tensor Solutions*, Springer Natural Hazards,
https://doi.org/10.1007/978-3-319-77359-9_13

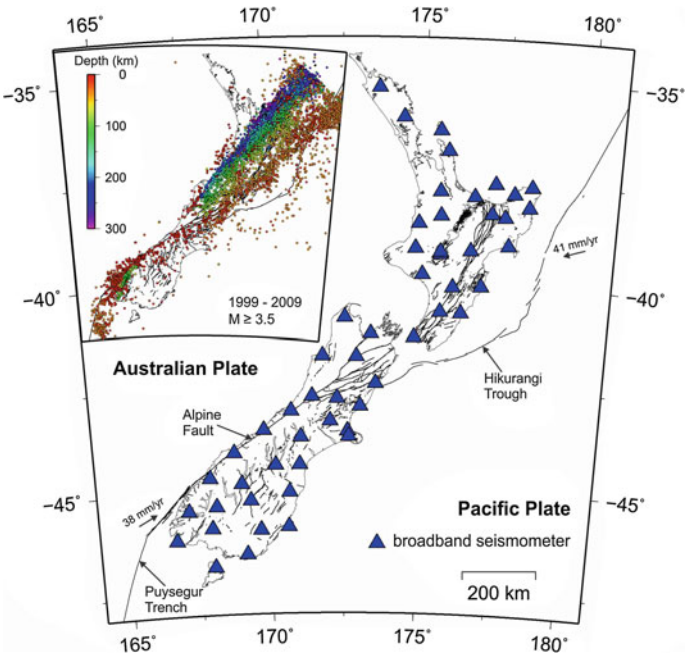

Fig. 1 New Zealand broadband seismometer network with more than 50 broadband seismometers available for calculating RMT solutions. New Zealand sits atop the boundary between the Pacific and Australian plates. (inset) 10 years of seismicity in New Zealand from (shown is $M \geq 3.5$). New Zealand seismicity ranges from earthquakes with surface ruptures to earthquakes several hundred kilometres deep beneath North Island. To represent New Zealand seismicity prior to the earthquake sequences discussed in this article, the 10 years shown spans the decade before the 15 July 2009 M_w 7.8 Dusky Sound earthquake

several hundred kilometres deep. There are also several active volcanoes present in central North Island and north of North Island. Beneath North Island, there is active subduction of the Pacific plate beneath the Australian plate at the Hikurangi trough which is capable of producing great ($M > 8.0$) megathrust earthquakes (e.g. Wallace et al. 2014; Clark et al. 2015). The Wellington region, the capital of New Zealand in southern North Island, is also at risk from shallow strike-slip earthquakes, notably the Wellington Fault which is capable of producing $M > 7.5$ earthquakes with recurrence intervals of 610–1100 years (e.g. Little et al. 2010; Langridge et al. 2011), and the Wairarapa Fault which last ruptured in 1855 with M 8.2 (e.g. Van Dissen and Berryman 1996; Rodgers and Little 2006).

At the southern end of South Island subduction polarity is reversed with the Australian plate subducting beneath the Pacific plate at the Puysegur Trench, which also produces earthquakes with a wide range of focal depths. The largest recorded earthquake at the Puysegur Trench was the 15 July 2009 M 7.8 Dusky Sound earthquake (Fry et al. 2010; Beavan et al. 2010). Between the two subduction zones is the Alpine

Fault, a 650 km long, right-lateral strike-slip fault forming the Pacific/Australian plate boundary. The Alpine Fault has ruptured in major earthquakes (M > 7.5) with recurrence intervals of ~300 years, with the last major earthquake occurring in 1717 (e.g. Cooper and Norris 1990; Berryman et al. 2012; Cochran et al. 2017). Earthquakes in central South Island are primarily within the overlying crust with focal depths < 40 km.

3 New Zealand Seismic Network

In 2001 the New Zealand Earthquake Commission (EQC) provided funding to GNS Science to launch the GeoNet project. The purpose of GeoNet is to upgrade the existing seismic network, provide data communication links, modernize data management practices, and introduce new initiatives for volcano surveillance, landslide response, earth deformation monitoring, and tsunami warning systems. GeoNet manages a large network of three-component broadband seismometers, strong-motion accelerometers, GPS sites, volcano surveillance equipment, and tsunami tide gauges. Figure 1 shows the broadband seismograph network in New Zealand with more than 50 three-component broadband sites across the country which are used for moment tensor analysis. Petersen et al. (2011) provides a detailed overview of the New Zealand seismic network.

4 Regional Moment Tensor Analysis

4.1 Moment Tensor Theory

Moment tensor analysis involves fitting theoretical waveforms with observed broadband waveforms and inverting for the moment tensor elements. A brief description of moment tensor theory is included here, and detailed descriptions of the theory and methodology are provided in a number of sources (e.g. Aki and Richards 1980; Jost and Herrmann 1989; Frohlich and Apperson 1992; other chapters in this volume). The general representation of a seismic source is given in Aki and Richards (1980) as

$$d_n(x,t) = \int_{-\infty}^{\infty} \int_{V} G_{nk}\left(x,t;r,\bar{t}\right) f_k\left(r,\bar{t}\right) dV(r)\, d\bar{t}, \tag{1}$$

where d_n is the observed displacement at an arbitrary position x at time t due to a distribution of equivalent body force densities f_k. G_{nk} are the components of the

Green's function containing the effects of the Earth structure, and V is the source volume. The problem can be discretised as

$$d_n(x,t) = \sum_{i=1}^{5} m_i * G_{in}, \tag{2}$$

where d_n is the vertical, radial, or transverse displacement, and m_i are the moment tensor elements with $m_1 = M_{11}$, $m_2 = M_{22}$, $m_3 = M_{12}$, $m_4 = M_{13}$, and $m_5 = M_{23}$ (note $M_{33} = -(M_{11} + M_{22})$). G_{in} are the Green's functions corresponding to each of the respective moment tensor elements. The Green's functions are usually calculated using simple 1-D velocity models appropriate to the source region; however, 2-D or 3-D models can also be used. Using the observed displacements d_n, and Green's functions G_n, the moment tensor elements can be inverted for, most commonly using a least-squares inversion that can be written as

$$d = G\overline{m}, \tag{3}$$

where d consists of n waveforms, G is an $n \times 6$ matrix consisting of the Green's functions, and $\overline{m}$ is the vector containing the moment tensor elements to be determined.

Moment tensor analysis of larger magnitude earthquakes ($M_w > 5.0$–5.5) at teleseismic distances ($\gtrsim$1000 km) has been ongoing since the late-1970s by the Global Centroid Moment Tensor (GCMT) Project (formerly Harvard CMT solutions; e.g. Dziewonski et al. 1981), and the United States Geological Survey (USGS; e.g. Sipkin 1986). Regional moment tensor (RMT) solutions differ from teleseismic methods in that they use regional data (source-receiver distances $\lesssim$ 1000 km) and velocity models specific to the source region to calculate Green's functions. RMT analysis for smaller magnitude earthquakes ($M_w < 5.0$–5.5) has become a routine technique with a number of agencies providing catalogues of RMT solutions (e.g. Bent 2015; Braunmiller and Nábelek 2002; Braunmiller et al. 2002; Clinton et al. 2006; Kao et al. 1998; Kao et al. 2012; Kubo et al. 2002; Ristau et al. 2007; Ristau 2013; Ruppert and Hansen 2010; Scognamiglio et al. 2009; Whidden and Pankow 2012).

5 Regional Moment Tensor Analysis in New Zealand

RMT solutions at GeoNet are calculated using the method developed by Doug Dreger at the University of California, Berkeley Seismological Laboratory (e.g. Dreger and Helmberger 1993; Pasyanos et al. 1996; Dreger 2003) for use on smaller magnitude earthquakes. Ristau (2008) introduced RMT analysis in New Zealand, provided the velocity models that were developed to calculate Green's functions, and outlined the procedure for calculating a RMT solution. Ristau (2008) showed examples of RMT solutions and compared them with GCMT (see Sect. 9) and first-motion solutions,

and discussed some the issues encountered in implementing the procedure. Prior to August 2003 the New Zealand broadband seismograph network was not sufficiently dense to calculate RMT solutions (Matcham et al. 2006).

GeoNet locates over 15 000 earthquakes each year in New Zealand and adjacent offshore regions (Fig. 1 *inset*). Detailed overviews of New Zealand seismicity can be found in Robinson (1986), Reyners (1989), Anderson and Webb (1994), and Ristau (2008). Typically, more than 1000 earthquakes each year have local magnitude (M_L) $\geq$ 3.5 which make them candidates for RMT analysis. In September 2012 GeoNet began using SeisComP3 (SC3) for earthquake analysis, replacing the CalTech-USGS seismic processor (CUSP) system which had been in use since 1986. Ristau (2009) showed there is a significant discrepancy between M_L calculated with CUSP and M_w for New Zealand earthquakes, with M_L normally being larger than M_w and the discrepancy being particularly large for deep focus (>33 km) earthquakes. Therefore, CUSP M_L often needs to be $\geq$~4.0 to calculate a moment tensor solution; however, it has been possible to calculate RMT solutions for some smaller events depending on the signal-to-noise ratio. SC3 M_L correlates better with M_w, and earthquakes with smaller SC3 M_L's are able to have moment tensor solutions calculated (Ristau et al. 2016).

Since RMT analysis was implemented by GeoNet in early-2007, more than 2000 RMT solutions have been calculated for earthquakes in New Zealand and adjacent offshore regions with M_w 3.2–7.4 and depth 2–375 km, with the catalogue beginning August 2003. The vast majority are for earthquakes in the range M_w 3.5–5.0; however, there are 34 earthquakes in the RMT catalogue with $M_w \geq 6.0$, with five having $M_w \geq 7.0$ (Fig. 2). This does not include two M_w 7.8 earthquakes that were too large to calculate reliable RMT solutions (the reasons are discussed later in this article).

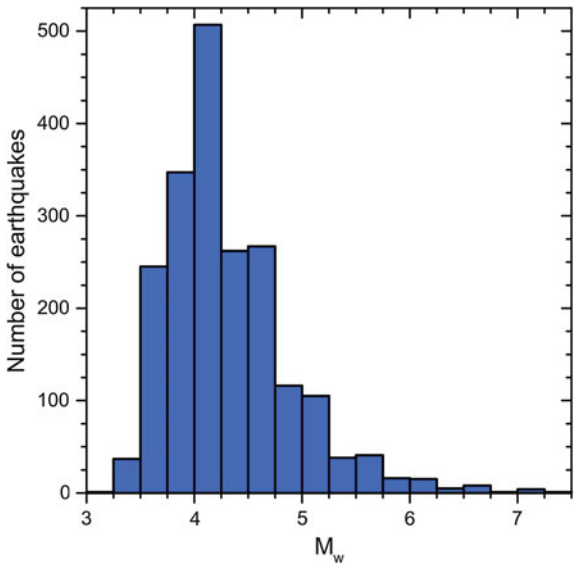

Fig. 2 M_w distribution of earthquakes in the RMT catalogue. Most earthquakes are in the range M_w 3.5–5.0; however, 34 have $M_w \geq 6.0$. The 15 July 2009 M_w 7.8 Dusky Sound and 13 November 2016 M_w 7.8 Kaikoura earthquakes are not included in this plot as they were too large to calculate reliable RMT solutions

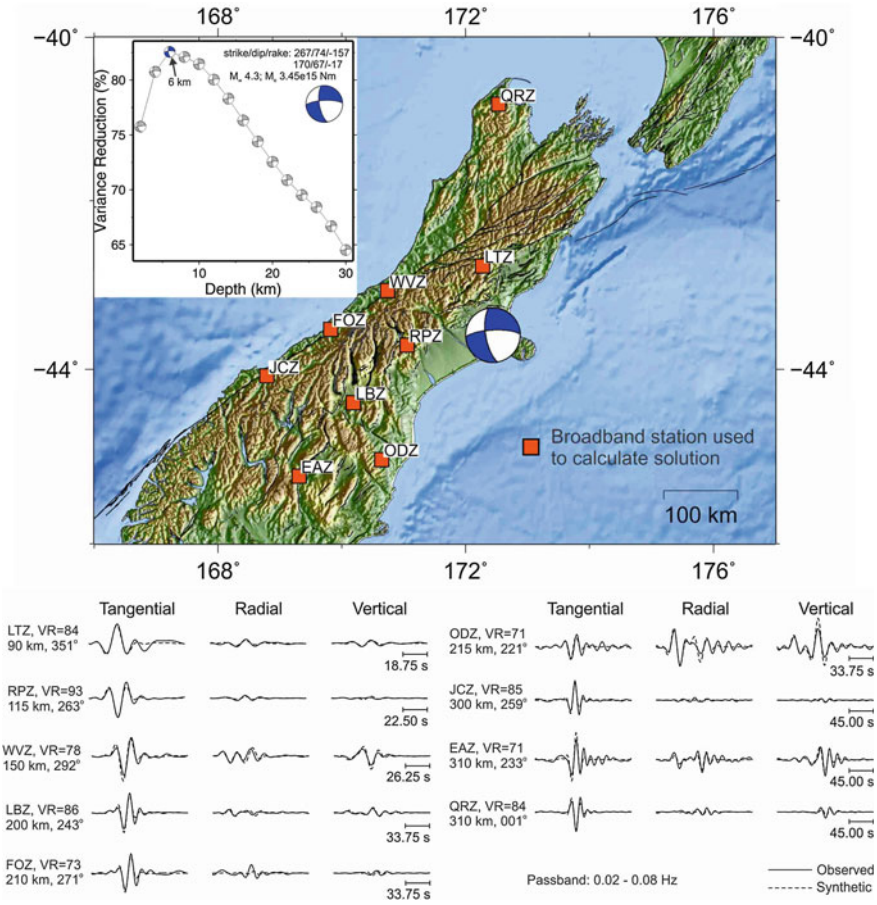

Fig. 3 Example of a RMT solution for a M_w 4.3 earthquake in the Canterbury region. (top) Map showing the focal mechanism and the nine broadband seismometers used to calculate the solution. (inset) Variance reduction versus centroid depth showing the best-fit at a depth of 6 km. (bottom) The waveforms were filtered using a passband of 0.02–0.08 Hz and there is a very good fit between the synthetic and observed waveforms

Figure 3 shows an example of a RMT solution for a M_w 4.3 earthquake in the Canterbury region of South Island. Reliable RMT solutions have been calculated using as few as three broadband stations; however, the average is around six stations. It is preferable to have stations with good azimuthal coverage, but in a region like New Zealand—a narrow country with many offshore earthquakes—this is often not possible.

The more than 2000 RMT solutions for New Zealand include RMT solutions from five significant earthquake sequences that have impacted New Zealand since July 2009 (Fig. 4). In chronological order these earthquake sequences are:

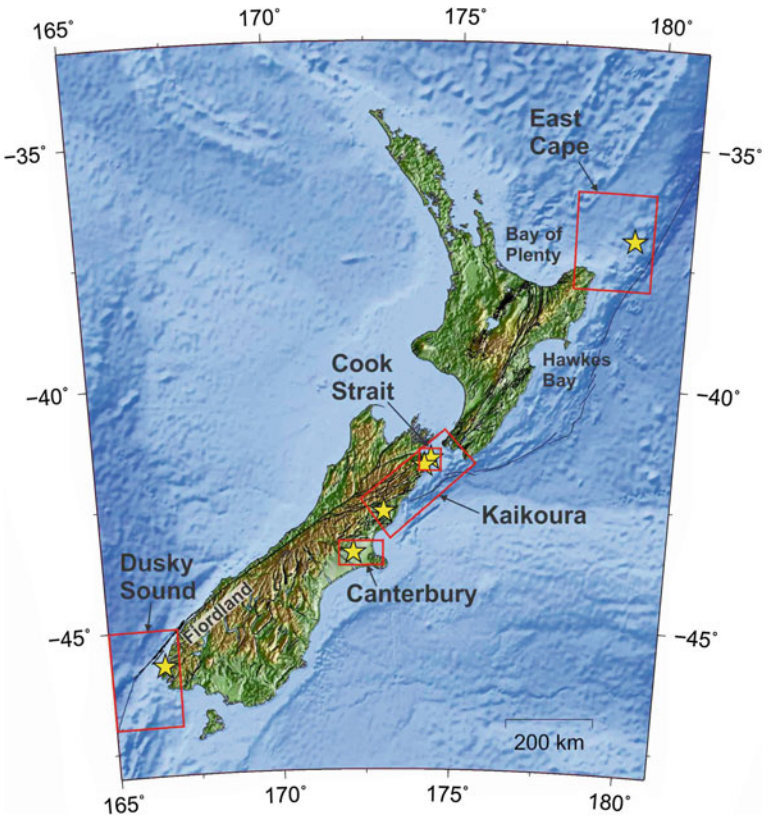

Fig. 4 Locations of the five significant earthquakes in New Zealand since July 2009 which are discussed in this article (yellow stars) and aftershock zones where RMT solutions were calculated (red boxes)

1. 15 July 2009 M_w 7.8, Dusky Sound, Fiordland (Fry et al. 2010; Beavan et al. 2010);
2. 3 September 2010 M_w 7.1, Darfield, Canterbury (Gledhill et al. 2011);
3. 21 July 2013 M_w 6.6 and 16 August 2013 M_w 6.6, Cook Strait (Hamling et al. 2014);
4. 1 September 2016 M_w 7.1, East Cape (Te Araroa) (Ristau 2017);
5. 13 November 2016 M_w 7.8, Kaikoura (Kaiser et al. 2017).

At the time this overview chapter was written the M_w 7.1 East Cape and M_w 7.8 Kaikoura earthquakes had recently occurred; therefore, much work is still needed to fully characterise these earthquakes and aftershock sequences.

6 Overview of New Zealand Moment Tensor Solutions

I will first provide an overview of New Zealand RMT solutions, excluding events associated with the five earthquake sequences mentioned above. Figure 5 shows RMT solutions for North Island and South Island, and adjacent offshore regions, separated into depth ≤ 33 km (left) and >33 km (right). In central North Island there is a band of shallow RMT solutions that extends to the Bay of Plenty region. These earthquakes are typically normal or strike-slip faulting with NW-SE oriented T-axes and reflect the influence of the Taupo rift zone (Seeback et al. 2014). Along the east coast of North Island and the offshore region, focal mechanisms are a mixture of strike-slip, reverse, and normal faulting. The two largest earthquakes in this region were in-slab, normal faulting earthquakes. The 20 December 2007 M_w 6.7 earthquake occurred near the city of Gisborne at a depth of 24 km and caused widespread minor damage

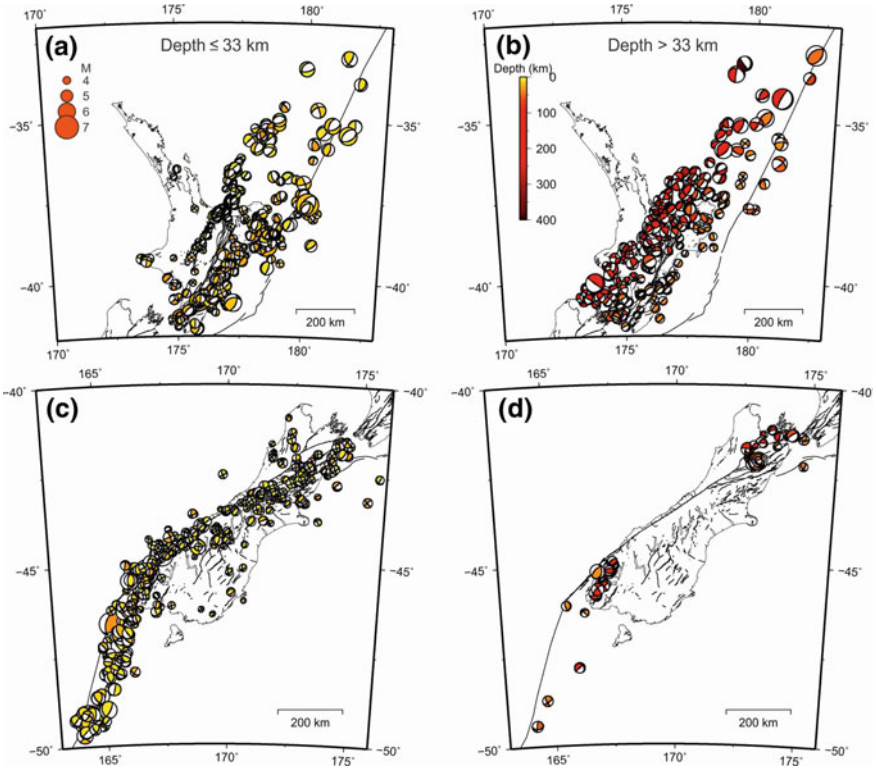

Fig. 5 RMT solutions for New Zealand, excluding earthquakes associated with the five earthquake sequences shown in Fig. 4. **a** RMT solutions for North Island for earthquakes with centroid depth ≤ 33 km. **b** RMT solutions for North Island earthquakes with centroid depth > 33 km. **c** RMT solutions for South Island for earthquakes with centroid depth ≤ 33 km. **d** RMT solutions for South Island earthquakes with centroid depth > 33 km

along with some structural damage (Holden et al. 2008). A similar earthquake struck on 16 November 2014 with M_w 6.8, but was located further offshore and resulted in less human impact. Two other significant earthquakes were the 20 January 2014 M_w 6.3 Eketahuna earthquake (e.g. Abercrombie et al. 2017), and the 20 January 2005 M_w 5.3 Upper Hutt earthquake (e.g. Reyners and Bannister 2007), with epicentres in southern North Island. These earthquakes were widely felt throughout southern North Island and caused widespread minor damage. Both earthquakes had normal faulting mechanisms at depths of ~20–30 km, consistent with being in-slab events. The deeper North Island earthquakes are also a mixture of normal, reverse, and strike-slip faulting; however, many of the deeper earthquakes are reverse faulting and related to subduction of the Pacific plate. The deep earthquakes can have $M_w \geq 6.0$ and be widely felt throughout North Island, but they typically do little damage due to their depth.

South Island has a different pattern of seismicity than North Island, with the majority of the seismic activity being dominated by the plate boundary between the Australian and Pacific plates, and the Alpine Fault delineating the boundary. The onshore shallow seismicity is almost all strike-slip or reverse faulting with P-axes consistently oriented ~115°. Further south, in the Fiordland region of the southwest South Island and south of South Island, the Puysegur subduction zone dominates with many reverse faulting focal mechanisms. The Fiordland region is the most seismically active region of New Zealand with 11 earthquakes $M_w \geq 6.0$ in the RMT catalogue; however, due to the sparse population in Fiordland the damage is typically minor. The 21 August 2003 M_w 7.1 Fiordland earthquake was the largest shallow earthquake in New Zealand in 35 years at the time, and was a reverse faulting event on the shallow part of the subduction interface (Reyners et al. 2003). The 15 October 2007 M_w 6.7 George Sound earthquake was centred northeast of the M_w 7.1 Fiordland earthquake, and was also a reverse faulting event on the subduction interface (Petersen et al. 2009). South of South Island a M_w 7.4 earthquake occurred on 30 September 2007 with a reverse faulting mechanism and may also have been on the subduction interface. This earthquake was followed by a M_w 6.6 aftershock. Central South Island is largely devoid of deep seismicity; however, there is some deeper seismic activity at the north end which marks the southern boundary of the Hikurangi subduction zone. In particular, near the town of Hanmer Springs at the northern end of South Island, there is a cluster of oblique faulting events, several with $M_w \geq 5.0$, at depths of ~60–70 km. There is deep seismic activity in the Fiordland region associated with the Puysegur subduction zone and the faulting style varies between strike-slip and reverse, but the vast majority have depths $\lesssim$150 km.

7 Discussion of Earthquake Sequences

7.1 Dusky Sound, Fiordland: 15 July 2009, M_w 7.8

The M_w 7.8 Dusky Sound earthquake was the largest earthquake in New Zealand since the 1931 M 7.8 Hawkes Bay earthquake, east coast of North Island (Fry et al. 2010; Beavan et al. 2010). The earthquake was a thrust faulting event on the subduction interface of the Puysegur subduction zone. Most of the energy release was at very low frequencies and, combined with the remote location of the epicentre, resulted in mainly minor damage. Using the focal mechanism of the mainshock, rupture area, and location of nearby faults, Coulomb stress models show a stress increase of ~0.2 MPa on the offshore extension of the Alpine Fault (Fry et al. 2010; Beavan et al. 2010).

The RMT method used at GeoNet assumes a point-source (i.e. a source with no dimensions), which is adequate when the wavelengths analysed are much greater than the source dimensions. For earthquakes less than M_w ~ 7.0–7.5 a point-source assumption is sufficient; however, for larger earthquakes the point-source assumption using the frequency bands and source-receiver distances normally used for RMT analysis no longer applies, and either more complex source modelling or very long wavelengths are needed. For the Dusky Sound earthquake most of the broadband seismometers in New Zealand saturated which made the data unusable for RMT analysis, and even the furthest stations (source-receiver distance ~1000 km), were not distant enough to utilise long enough wavelengths to calculate a reliable RMT solution for the mainshock. Therefore, the W-phase teleseismic moment tensor solution calculated by the USGS is used for the mainshock (see Sect. 9).

132 RMT solutions for aftershocks were calculated, with the largest being M_w 6.1 (Fig. 6). The shallowest solutions (Fig. 6a) are mainly normal faulting mechanisms with one near-vertical fault plane and one near-horizontal fault plane. In the 7–12 km depth range (Fig. 6b) the mechanisms are mainly reverse or strike-slip faulting with a P-axis oriented approximately E-W, similar to the mainshock. Many of the strike-slip faulting mechanisms are located near the offshore extension of the Alpine Fault. However, given the uncertainty in epicentres in the Fiordland region it is not clear whether these aftershocks are on the Alpine Fault and induced by the Dusky Sound earthquake, or on structures near the Alpine Fault. At 13–19 km (Fig. 6c) the mechanisms are mainly reverse faulting and very similar to the mainshock; therefore, they may have also occurred on the plate interface. At 20–30 km (Fig. 6d) the mechanisms are a mixture of reverse, normal, and strike-slip faulting suggesting that the tectonic setting at greater depths becomes more complicated. Some aftershocks may be occurring in the crust above the plate interface and others within the subducting plate.

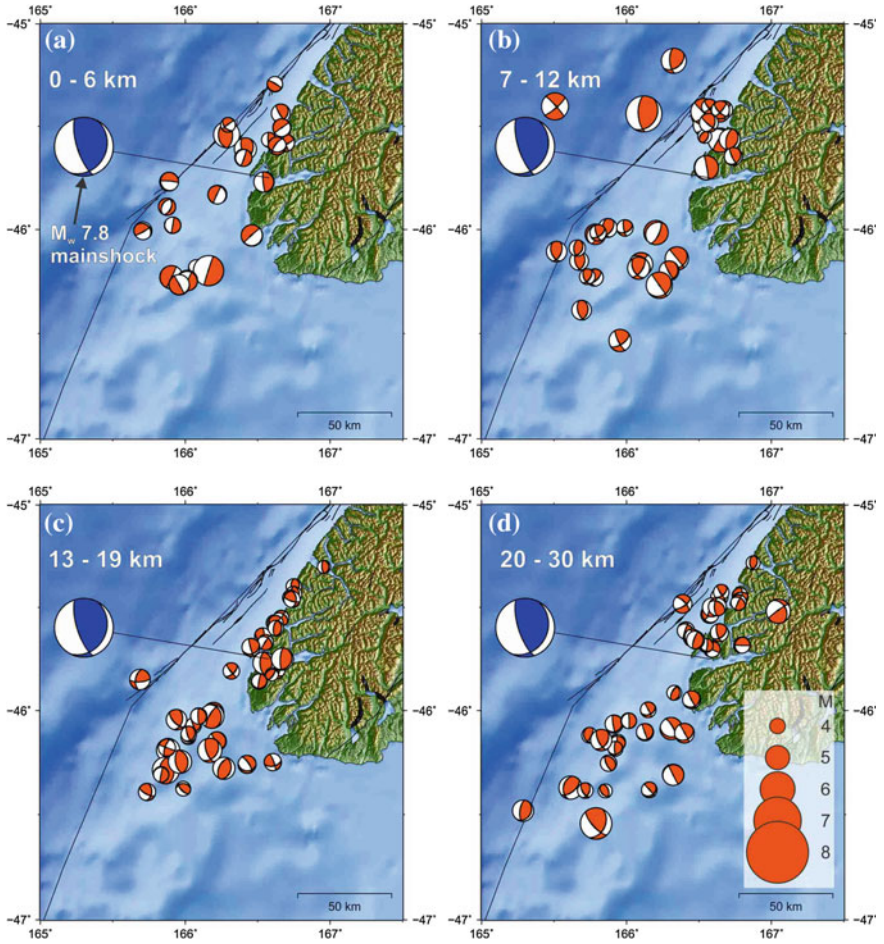

Fig. 6 RMT solutions for aftershocks of the Dusky Sound earthquake. The mainshock, taken from the USGS W-phase solution, is the blue focal mechanism, and aftershocks are orange focal mechanisms. **a** Focal mechanisms for aftershocks with depth 0–6 km. **b** Focal mechanisms for aftershocks with depth 7–12 km. **c** Focal mechanisms for aftershocks with depth 13–19 km. **d** Focal mechanisms for aftershocks with depth 20–30 km

7.2 Darfield, Canterbury: 3 September 2010, M_w 7.1

The M_w 7.1 Darfield earthquake occurred in the Canterbury region of New Zealand, ~10 southeast of the town of Darfield and ~40 km west of Christchurch, New Zealand's second largest city (population ~377 000) (Gledhill et al. 2011). The earthquake was widely felt throughout South Island and southern North Island, with over 7300 felt reports received, and caused significant damage in Christchurch, with maximum intensity MM 9 in the epicentral region. Through a fortunate combination

of strict building codes and the earthquake occurring on a Saturday at 04:35 NZST when the streets were largely deserted, there were no deaths and only two serious injuries. On 21 February 2011 (~5½ months after the Darfield earthquake) the M_w 6.2 Christchurch earthquake struck as an aftershock to the Darfield earthquake (Kaiser et al. 2012). The Christchurch earthquake struck ~6 km southeast of the city centre beneath the outer suburbs of Christchurch at shallow depth. In contrast to the Darfield earthquake, the Christchurch earthquake struck at 12:51 NZST on a weekday when the city centre was at its most populated. Severe building damage was widespread and resulted in 185 fatalities, many of which occurred with the collapse of the multi-story Canterbury Television and Pyne Gould buildings. The aftershock sequence has continued for years, with the most recent significant aftershock being M_w 5.8 on 14 February 2016.

Before the Darfield earthquake, the Canterbury region had a historically low level of seismic activity compared with many other parts of New Zealand. As a result, an earthquake similar to Darfield was considered a low-probability event for New Zealand, although the possibility of a comparable earthquake had been acknowledged in seismic hazard models (Stirling et al. 2012). Most of the moment release was along the previously unknown Greendale Fault which had not ruptured for 18 000–20 000 years. Geodetic and strong-motion modelling (e.g. Holden and Beavan Holden and Beavan 2012; Beavan et al. 2012) identified at least seven individual fault segments which were active during the earthquake, including a blind reverse fault several kilometres north of the Greendale Fault where the rupture initiated.

The Darfield earthquake is an important case study on how regional and teleseismic moment tensor solutions can differ significantly as a result of the methods used to calculate them. The teleseismic moment tensor solutions calculated by the USGS and Global CMT Project (see Sect. 9) have a strike-slip focal mechanism consistent with the surface rupture of the Greendale Fault (Fig. 7a). In contrast, the GeoNet RMT solution and GeoNet first-motion solution indicated reverse faulting on either a shallow NW-dipping plane or a steep SE-dipping plane (Fig. 7a). As a result of the high density of strong-motion stations in the vicinity of the mainshock, the hypocentre was well constrained about 4 ± 0.5 km north of the surface trace of the Greendale Fault (Gledhill et al. 2011). Due to the well-constrained hypocentre with an estimated depth of about 11 km, the discrepancy between the hypocentre location and the trace of the Greendale Fault cannot be explained by the location uncertainty. A shallow-dipping fault plane could account for the discrepancy, but there should be near co-incidence of the epicentre with the trace of the Greendale Fault for any near-vertical strike-slip mechanism as indicated in the teleseismic moment tensor solutions.

Teleseismic moment tensor methods use lower frequency bands and much greater source-receiver distances than RMT methods. As a result, they are not able to resolve distinct mechanisms but instead provide an average over the whole event, which is dominated in the case of the Darfield earthquake by strike-slip movement along the Greendale Fault. The RMT solution uses higher frequency bands and smaller source-receiver distances, ~300–860 km for the GeoNet Darfield RMT solution, which makes the solution more sensitive to small-scale features. As a result, the

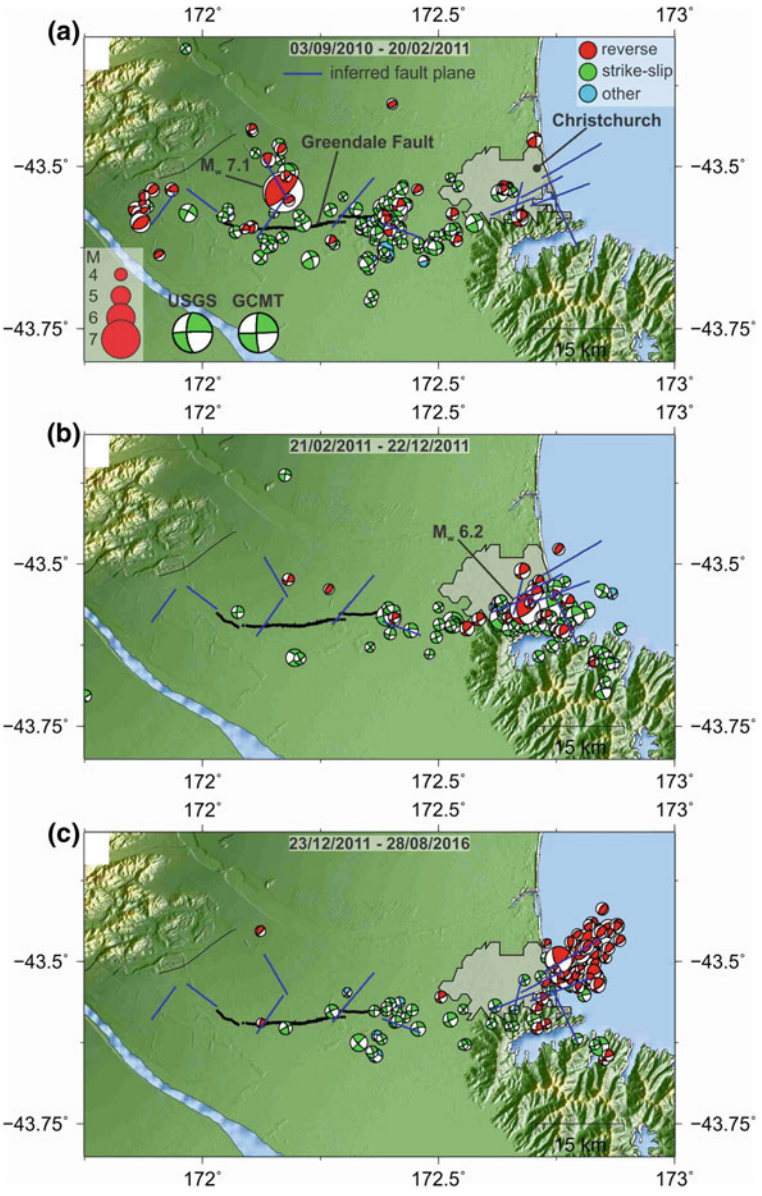

Fig. 7 RMT solutions for the Canterbury earthquake sequence. **a** The M_w 7.1 Darfield earthquake and aftershocks up to 20 February 2011. Also shown are the USGS and GCMT focal mechanisms for the mainshock showing strike-slip faulting as opposed to reverse faulting for the RMT solution. Focal mechanisms are colour-coded according to faulting style. Also shown in the surface fault trace of the Greendale Fault and inferred fault planes from geodetic studies. **b** The M_w 6.2 Christchurch earthquake and aftershocks up to 22 December 2011. **c** The 23 December 2011 Pegasus Bay aftershock sequence and aftershocks up to 28 August 2016, including the 14 February 2016 M_w 5.8 aftershock

GeoNet RMT solution models the nature of the initial reverse-faulting rupture. This demonstrates how, in the case of a complex rupture like the Darfield earthquake, the teleseismic and RMT focal mechanisms can be quite different from one another, but both are correct within the limitations of the methods used to calculate them.

Nearly 15 000 aftershocks have been recorded in the Canterbury/Christchurch region since the Darfield earthquake, and 378 RMT solutions have been calculated with M_w 3.4–6.2. Figure 7 separates the RMT solutions into three groups based on the main earthquakes in the Canterbury sequence. In Fig. 7a are the RMT solutions from the 3 September 2010 Darfield earthquake up to the 21 February 2011 Christchurch earthquake; Fig. 7b from the 21 February 2011 Christchurch earthquake up to the 23 December 2011 Pegasus Bay aftershock sequence; Fig. 7c from the 23 December 2011 Pegasus Bay aftershock sequence to 28 August 2016.

In Fig. 7a, focal mechanisms from 153 RMT solutions show a variety of faulting styles, providing evidence for the complex nature of the rupture process. Focal mechanisms in the immediate area of the initial rupture are a mixture of reverse and strike-slip faulting. At the western end of the fault zone the mechanisms are predominantly reverse faulting, consistent with the geodetic model of the main rupture, which includes a reverse faulting segment at the western end of the rupture zone. East of the main rupture zone, leading into Christchurch, focal mechanisms are mainly reverse faulting or oblique-reverse faulting.

The aftershock locations mostly coincide with the Greendale Fault trace and the location of inferred subsurface faults. However, at the eastern end of the Greendale Fault there is a NE-SW trend of aftershocks that are not associated with any known subsurface fault, and this is particularly noticeable in the plot of focal mechanisms. Further east there is another NE-SW trend of aftershocks between the Greendale Fault and Christchurch that is also not associated with any known subsurface fault, and in this region the focal mechanisms change from mainly strike-slip faulting in the west to oblique-reverse faulting closer to Christchurch.

On 26 December 2010 NZST (25 December 2010 UTC) a cluster of very shallow aftershocks occurred near the Christchurch city centre. The largest, M_w 4.7, occurred at 12:30 NZST when the city centre was highly populated (Ristau 2011). These aftershocks were widely felt and the M_w 4.7 event caused damage to brick and masonry structures already weakened in the city centre. Three RMT solutions were calculated for events in the series of aftershocks, all with strike-slip mechanisms. Ristau (2011) also calculated 16 first-motion focal mechanism for events in this series, including the three events for which RMT solutions had been calculated, and although the first-motion solutions were for mainly reverse faulting, the P-axis orientation is consistent with those in the RMT solutions.

Figure 7b shows 113 focal mechanisms beginning with the 21 February 2011 M_w 6.2 Christchurch earthquake. The Christchurch earthquake occurred on a previously unmapped NE-SW striking fault in the Port Hills area of the outer suburbs of Christchurch (Fig. 7b), in an area of small positive stress increase resulting from the Darfield earthquake (Kaiser et al. 2012). The RMT solution shows primarily reverse faulting with a strike-slip component, consistent with the complex nature of

the faulting as indicated by the geodetic modelling which requires two, and possibly three faults to be active (Beavan et al. 2012). The earthquake triggered a rejuvenated aftershock sequence centred around Christchurch and into Pegasus Bay east of Christchurch, most notably a M_w 6.0 aftershock on 13 June 2011. The 13 June 2011 aftershock was a strike-slip event that occurred ~4 km east of the Christchurch earthquake epicentre (Fig. 7b) and also involved at least two fault ruptures (Beavan et al. 2012). Following the 13 June 2011 aftershock many of the aftershocks extended SE into Banks Peninsula where little aftershock activity had occurred previously. Whereas the Christchurch earthquake had mainly reverse faulting, focal mechanism derived from RMT solutions for aftershocks to the Christchurch earthquake indicated mainly strike-slip faulting, although there were some with reverse or oblique-reverse faulting (Fig. 7b).

Three earthquakes on 23 December 2011 UTC (M_w 5.4–5.9) centred near Pegasus Bay, east of Christchurch, triggered a NE-SW series of aftershocks that extended offshore (Fig. 7c). These earthquakes were widely felt in Christchurch but damage was minimal due to their offshore location (Ristau et al. 2013). 53 RMT solutions were determined for events in Pegasus Bay with a majority (45 of 53) indicating reverse or oblique-reverse faulting. This is in contrast with the rest of the Canterbury aftershock sequence where ~74% of the focal mechanism indicated strike-slip faulting (Ristau et al. 2013). Pegasus Bay was also the location of the most recent significant aftershock in the Canterbury sequence, a M_w 5.8 oblique-reverse faulting event on 14 February 2016 (Herman and Furlong 2016).

7.3 Cook Strait/Lake Grassmere: 21 July 2013, M_w 6.6 and 16 August 2013, M_w 6.6

The Cook Strait and Lake Grassmere earthquakes of July and August 2013 was an earthquake doublet—two earthquakes with similar epicentre, magnitude, and source properties that occur closely spaced in time (Hamling et al. 2014; Holden et al. 2013). Cook Strait is a narrow strait that separates North Island and South Island, and Lake Grassmere is near the town of Seddon at the northern end of South Island. The earthquakes were ~50–70 km southwest of New Zealand's capital, Wellington. The earthquakes were widely felt throughout northern South Island and southern North Island, and caused significant structural damage in northern South Island communities and significant non-structural damage in the greater Wellington region.

The sequence began with two foreshocks of M_w 5.5 on 18 July 2013 and M_w 5.8 on 20 July 2013 (Fig. 8). The foreshocks were located in Cook Strait and were both reverse faulting mechanisms with depths ~20 km. Most of the RMT solutions for aftershocks to the foreshocks were also reverse faulting mechanisms with similar depth. On 21 July 2013 the M_w 6.6 Cook Strait earthquake struck with over 5500 felt reports, mostly from North Island and northern South Island. The Cook Strait earthquake was a right-lateral strike-slip earthquake at a depth of ~20 km along a

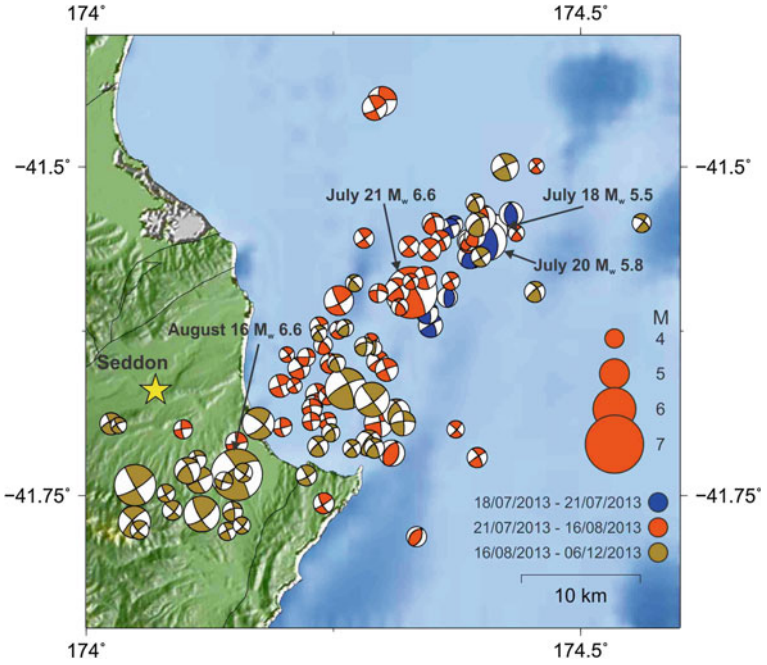

Fig. 8 RMT solutions for the Cook Strait/Lake Grassmere earthquake sequence. Focal mechanisms are colour-coded by time with blue mechanisms corresponding to foreshocks to the Cook Strait earthquake, orange mechanisms for the M_w 6.6 Cook Strait earthquake and aftershocks, and gold mechanisms for the M_w 6.6 Lake Grassmere earthquake and aftershocks. The town of Seddon is shown by the yellow star

previously unmapped offshore fault. RMT solutions for aftershocks were predominantly strike-slip with most located SW of the mainshock towards South Island. The depths of the RMT solutions trend towards shallower depths as they get closer to South Island.

On 16 August 2013 the M_w 6.6 Lake Grassmere earthquake occurred with nearly 6200 felt reports from North Island and northern South Island. This earthquake was also a right-lateral strike-slip earthquake, very similar to the earlier Cook Strait earthquake. As a result of their similar source properties, magnitudes, epicentres, and occurring less than a month apart they can be considered an earthquake doublet. Geodetic modelling and Coulomb stress analysis suggest that the Lake Grassmere earthquake was triggered by the Cook Strait earthquake, which in turn was triggered by the earlier foreshocks (Hamling et al. 2014). As with the Cook Strait earthquake, most of the RMT solutions for Lake Grassmere aftershocks are strike-slip faulting but with shallower depths.

Northern South Island, Cook Strait, and southern North Island have a large number of active faults, and the region sit atop the Hikurangi subduction zone. Slip models derived using focal mechanism information can be used to resolve Coulomb stress

transfer onto nearby mapped faults. One of the most important faults with a positive stress change following the Cook Strait/Lake Grassmere sequence is the southern extension of the Wellington Fault which showed a positive stress change of ~0.1 MPa (Hamling et al. 2014). The Wellington Fault extends through the heart of the Wellington city centre and north to the populated Hutt Valley, and is capable of rupturing in M > 7.5 earthquakes with a recurrence interval of 610–1100 years (Little et al. 2010; Langridge et al. 2011). The second area of concern is the Hikurangi subduction zone which has the potential to rupture in M > 8.0 earthquakes (Wallace et al. 2014; Clark et al. 2015). Hamling et al. (2014) concluded that it is likely that the Cook Strait and Lake Grassmere earthquakes resulted in a positive stress change approaching 0.3 MPa on the Hikurangi plate interface.

7.4 East Cape: 1 September 2016, M_w 7.1

The M_w 7.1 East Cape (Te Araroa) earthquake occurred ~125 km NE of East Cape, at the northeast end of North Island (Fig. 9). The offshore epicentre resulted in mainly minor damage; however, GeoNet received more than 4700 felt reports from across North Island and northern South Island. A minor tsunami of ~30 cm was recorded at the East Cape and Great Barrier Island tide gauges, and many local residents self-evacuated to higher ground when they felt strong shaking that lasted for more than 30 s.

The earthquake was preceded by a M_w 5.8 foreshock on 31 August 2016, which was a normal faulting mechanism with one high angle and one low angle fault plane, at a depth of 15 km (Fig. 9). The mainshock was an oblique-normal faulting mechanism with one high angle and one low angle fault plane, but deeper at 23 km. Initially a tsunami was not anticipated due to the magnitude, depth, and faulting style, and it was not until it was detected at tide gauges that it was known a tsunami had been generated. RMT solutions have been calculated for 27 aftershocks with M_w 4.4–6.0 and depths 6–24 km. Due to the complex nature of the local crustal structure and the offshore location, it was not possible to calculate reliable RMT solutions for smaller aftershocks. The aftershocks have similar mechanisms to the foreshock and mainshock, and almost all are located southwest of the mainshock and at shallower depth (Fig. 9). One notable exception is the largest aftershock (M_w 6.0) which was located east of the mainshock. With the uncertainty in the hypocentre of the mainshock it is not clear how the East Cape earthquake relates to the plate interface. The centroid depth of 23 km is consistent with the depth of the plate interface in the hypocentral region, but there is currently no evidence of rupture on the interface.

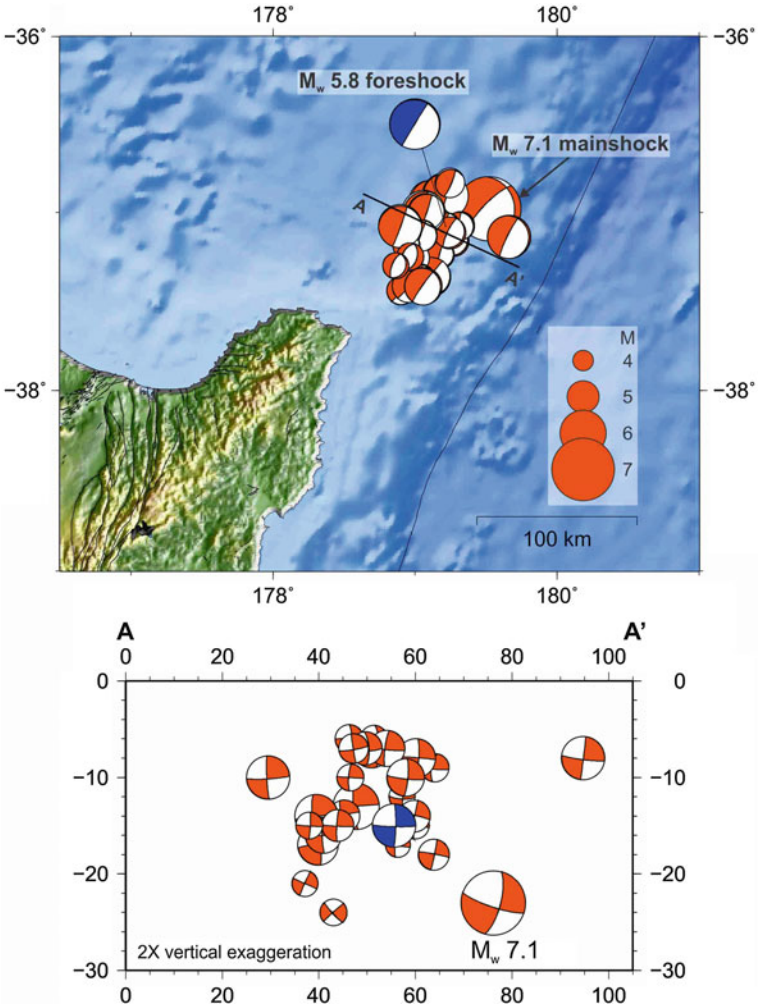

Fig. 9 (top) RMT solutions for the East Cape earthquake and aftershocks. The blue mechanism is the M_w 5.8 foreshock which occurred the day before the mainshock. (bottom) Cross-section showing aftershocks located shallower and west of the mainshock. The exception is the largest aftershock (M_w 6.0) which was located east of the mainshock

7.5 Kaikoura: 13 November 2016, M_w 7.8

The M_w 7.8 Kaikoura earthquake occurred just past midnight NZST with an epicentre ~30 km from the northeast coast of South Island, near the town of Waiau. This was the largest earthquake in New Zealand since the 15 July 2009 M_w 7.8 Dusky Sound earthquake, and GeoNet received more than 15 800 felt reports from almost

all parts of the country. Heavy damage was experienced in the epicentral region, and widespread structural damage was reported in Wellington and Christchurch. One death resulted as a result of a collapsed house, and another from a heart attack. More than 100 000 landslides have been documented, and a tsunami of ~2 m was recorded on the closest tide gauge (Kaikoura); however, field observations show >4 m tsunami in some areas.

Almost every broadband seismometer in New Zealand saturated making it impossible to calculate a RMT solution for the mainshock. Teleseismic moment tensor solutions (USGS; GCMT; GFZ) showed mainly reverse faulting at a depth of ~10 km, and the rupture propagated north of the epicentre (Fig. 10). Geodetic and strong-motion modelling, along with field observations, show surface rupture on at least 12 different faults (Duputel and Rivera 2017; Hamling et al. 2017), and the earthquake involved at least 21 faults with the Kekerengu Fault showing up to 10–12 m of dextral slip (Kaiser et al. 2017). Although the teleseismic moment tensor solutions have a reverse faulting mechanism, they all have a significant non-double-couple component which could suggest a complex source. Fault motion from GPS and strong-motion modelling is a mixture of strike-slip and reverse faulting which may explain the large non-double-couple component in the moment tensor solutions. The rupture propagated above the southern end of the Hikurangi subduction zone and it is currently unclear how much, if any, of the plate interface was involved.

RMT solutions have been calculated for 213 aftershocks, including four with $M_w \geq 6.0$ (Fig. 10). Similar to the Canterbury aftershock sequence, the focal mechanisms show a variety of faulting styles providing evidence for the complex nature of the rupture process. Three of the $M_w \geq 6.0$ aftershocks have strike-slip mechanisms, with the largest (M_w 6.5) possibly associated with the Hundalee Fault. The second largest aftershock (M_w 6.3) has a thrust mechanism and may be associated with the Jordan Thrust Fault. The aftershock zone extends for ~230 km, with the northern end falling in the same region as the 2013 Cook Strait/Lake Grassmere earthquake sequence. The northern end of the aftershock zone approaches to within ~15 km of the south coast of the Wellington region. Over the entire aftershock zone, the RMT solutions have approximately equal numbers of reverse and strike-slip focal mechanisms. However, there appear to be two groups of aftershocks based on focal mechanism and depth. In the south (Fig. 10, orange) there are more reverse than strike-slip mechanisms, while to the north (Fig. 10, gold) there are more strike-slip than reverse mechanisms. The northern focal mechanisms are ~5 km deeper on average than the southern focal mechanisms.

8 Summary and Conclusions

Since routine RMT analysis for New Zealand earthquakes was implemented in early-2007, more than 2000 RMT solutions have been calculated with the catalogue beginning August 2003. The RMT solutions have made important contributions to

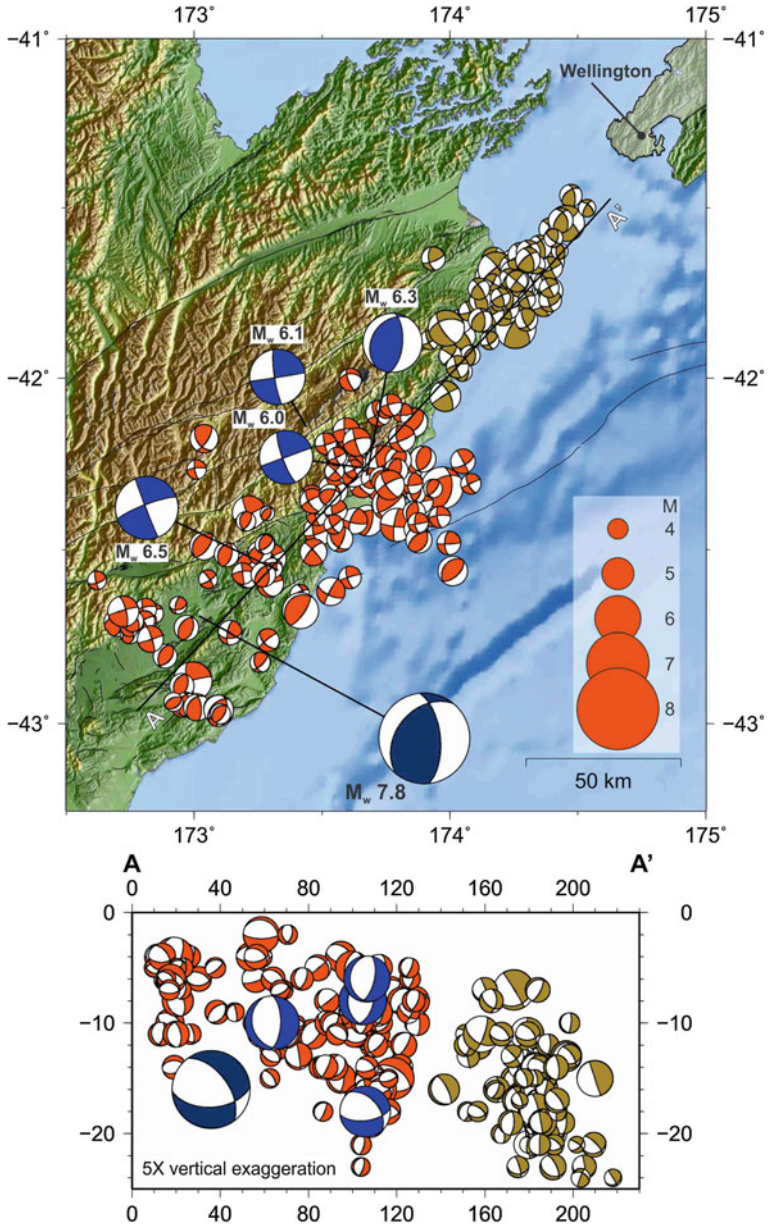

Fig. 10 (top) RMT solutions for aftershocks of the Kaikoura earthquake. The mainshock, taken from the USGS W-phase solution, is shown in dark blue, and the $M_w \geq 6.0$ aftershocks are shown in blue. The orange mechanisms are the southern group which have more reverse faulting than strike-slip faulting, and the gold mechanisms are the northern group which have more strike-slip faulting than reverse faulting. The northern end of the aftershock zone is ~15 km SW of the south coast of Wellington. (bottom) Cross-section showing the centroid depths becoming deeper from south-to-north Focal mechanism colours are the same as in map view

the understanding of the active tectonics and seismic hazard of New Zealand. The RMT catalogue includes solutions from five earthquake sequences that significantly impacted New Zealand since July 2009 and account for ~40% of the catalogue. The RMT solutions have helped to characterise the aftershock sequences and understand how they evolve over time.

RMT solutions are valuable for a variety of seismological and tectonic research topics. The improved magnitude estimates from using M_w are important for seismic hazard and risk studies, including calculating aftershock forecasts (e.g. Gerstenberger et al. 2012). The focal mechanisms are used to better understand stress transfer resulting from large earthquakes (e.g. Ellis et al. 2016), and for improved models of estimated shaking which can be used to direct resources for emergency response (e.g. Horspool et al. 2015). RMT solutions are also used to study regional scale tectonic stress and strain orientations (e.g. Ristau et al. 2007; Holt et al. 2013; Townend et al. 2012). RMT solutions are often needed to perform simulations for 3D seismic wave propagation, which can be used to validate and improve a local 3D velocity model (e.g. Loubet et al. 2016). RMT solutions can also be used to constrain the source geometry of a large earthquake in the case of complex ruptures where finite-fault inversion initially struggles to find the correct fault geometry (e.g. Gledhill et al. 2011).

9 Data and Resources

The regional moment tensor solutions used are calculated as part of the GNS Science GeoNet project (http://www.geonet.org.nz/). A complete list is available at http://info.geonet.org.nz/display/appdata/Earthquake+Catalogue (last updated 1 March 2016). The Global Centroid Moment Tensor Project (GCMT) database was searched using http://www.globalcmt.org/CMTsearch.html (last accessed 27 March 2017). The United States Geological Survey (USGS) earthquake database was searched using http://earthquake.usgs.gov/earthquakes/search/ (last accessed 27 March 2017). TheGeoForschungsZentrum(GFZ) moment tensor database was searched using https://eqarchives.wordpress.com/gfz-moment-tensors/ (last accessed 27 March 2017).

Acknowledgements Caroline Holden and Yoshihiro Kaneko provided many valuable comments which helped improve this article. Many of the figures were created using Generic Mapping Tools (GMT; Wessel and Smith 1998). Regional moment tensor solutions were computed using the mtpackagev1.1 package developed by Doug Dreger of the Berkeley Seismological Laboratory, and Green's functions were computed using the FKRPROG software developed by Chandan Saikia of URS.

References

Abercrombie RE, Bannister S, Ristau J, Doser D (2017) Variability of earthquake stress drop in a subduction setting, the Hikurangi margin, New Zealand. Geophys J Int 208:306–320. https://doi.org/10.1093/gji/ggw393

Aki K, Richards PG (1980) Quantitative seismology. W.H. Freeman and Co., San Francisco, p 932

Anderson H, Webb T (1994) New Zealand seismicity: patterns revealed by the upgraded national seismograph network. NZ J Geol Geophys 37:477–493

Beavan J, Samsonov S, Denys P, Sutherland R, Palmer N, Denham M (2010) Oblique slip on the Puysegur subduction interface in the 2009 July M_w 7.8 Dusky Sound earthquake from GPS and InSAR observations: implications for the tectonics of southwestern New Zealand. Geophys J Int 183:1265–1286. https://doi.org/10.1111/j.1365-246X.2010.04798.x

Beavan J, Motagh M, Fielding E, Donnelly N, Collett D (2012) Fault slip models of the 2010–2011 Canterbury, New Zealand, earthquakes from geodetic data, and observations of post-seismic ground deformation. NZ J Geol Geophys 55:207–221. https://doi.org/10.1080/00288306.2012.697472

Bent AL (2015) Regional centroid moment tensor solutions for eastern Canadian earthquakes: 2014. Geological Survey of Canada, Open File 7834, 35 p. https://doi.org/10.4095/296795

Berryman KR, Cochran UA, Clark KJ, Biasi GP, Langridge RM, Villamor P (2012) Major earthquakes occur regularly on an isolated plate boundary. Science 336:1690–1693. https://doi.org/10.1126/science.1218959

Braunmiller J, Nábělek J (2002) Seismotectonics of the explorer region. J Geophys Res 107:ETG1-1–ETG1-25. https://doi.org/10.1029/2001jb000220

Braunmiller J, Kradolfer U, Baer M, Giardini D (2002) Regional moment tensor determination in the European-Mediterranean area—initial results. Tectonophysics 356:5–22

Clark KJ, Hayward BW, Cochran UA, Wallace LM, Power WL, Sabaa AT (2015) Evidence for past subduction earthquakes at a plate boundary with widespread upper plate faulting: southern Hikurangi margin, New Zealand. Bull Seismol Soc Am 105:1661–1690. https://doi.org/10.1785/0120140291

Clinton JF, Hauksson E, Solanki K (2006) An evaluation of the SCSN moment tensor solutions: robustness of the M_w magnitude scale, style of faulting, and automation of the method. Bull Seismol Soc Am 96:1689–1705. https://doi.org/10.1785/0120050241

Cochran UA, Clark KJ, Howarth JD, Biasi GP, Langridge RM, Villamor P, Berryman KR, Vandergoes MJ (2017) A plate boundary record from a wetland adjacent to the Alpine Fault in New Zealand refines hazard estimates. Earth Planet Sci Lett 464:175–188. https://doi.org/10.1016/j.epsl.2017.02.026

Cooper AF, Norris RJ (1990) Estimates for the timing of the last coseismic displacement on the Alpine Fault, northern Fiordland, New Zealand. NZ J Geol Geophys 33:303–307

Dreger D, Helmberger DV (1993) Determination of source parameters at regional distances with single station or sparse network data. J Geophys Res 98:8107–8125

Dreger DS (2003) TDMT_INV: time domain seismic moment tensor INVersion. In: Lee WK (ed) International Handbook of earthquake and engineering seismology, vol 81B. Academic Press, Boston, p 1627

Duputel Z, Rivera L (2017) Long-period analysis of the 2016 Kaikoura earthquake. Phys Earth Planet Inter 265:62–66. https://doi.org/10.1016/j.pepi.2017.02.004

Dziewonski AM, Chou T-A, Woodhouse JH (1981) Determination of earthquake source parameters from waveform data for studies of global and regional seismicity. J Geophys Res 86:2825–2852

Ellis SM, Williams CA, Ristau J, Reyners ME, Eberhart-Phillips D, Wallace LM (2016) Calculating regional stresses for northern Canterbury: the effect of the 2010 Darfield earthquake. NZ J Geol Geophys 59:202–212. https://doi.org/10.1080/00288306.2015.1123740

Frohlich C, Apperson KD (1992) Earthquake focal mechanisms, moment tensors, and the consistency of seismic activity near plate boundaries. Tectonics 11:279–296

Fry B, Bannister SC, Beavan RJ, Bland L, Bradley BA, Cox SC, Cousins WJ, Gale NH, Hancox GT, Holden C, Jongens R, Power WL, Prasetya G, Reyners ME, Ristau J, Robinson R, Samsonov S, Wilson KJ, The GeoNet team (2010) The M_w 7.6 Dusky Sound earthquake of 2009: preliminary report. Bull NZ Soc Earthq Eng 43:24–40

Gerstenberger MC, Fry B, Abercrombie R, Doser D, Ristau J (2012) On the relation of stresses to aftershock decay. p 365. In: SSA 2012 annual meeting announcement Albany, California: Seismological Society of America. Seismol Res Lett *83*

Gledhill K, Ristau J, Reyners M, Fry B, Holden C (2011) The Darfield (Canterbury, New Zealand) M_w 7.1 earthquake of September 2010: a preliminary seismological report. Seismol Res Lett 82:378–386. https://doi.org/10.1785/gssrl.82.3.378

Hamling IJ, D'Anastasio E, Wallace LM, Ellis SM, Motagh M, Samsonov S, Palmer NG, Hreinsdottir S (2014) Crustal deformation and stress transfer during a propagating earthquake sequence: the 2013 Cook Strait sequence, central New Zealand. J Geophys Res 119:6080–6092. https://doi.org/10.1002/2014JB011084

Hamling IJ, Hreinsdóttir S, Clark K, Elliot J, Liang C, Fielding E, Litchfield N, Villamor P, Wallace L, Wright TJ, D'Anastasio E, Bannister S, Burbridge D, Denys P, Gentle P, Howarth J, Mueller C, Palmer N, Pearson C, Power W, Barnes P, Barrell DJA, Van Dissen R, Langridge R, Little T, Nicol A, Pettinga J, Rowland J, Stirling M (2017) Complex multifault rupture during the 2016 M_w 7.8 Kaikoura earthquake, New Zealand. Science. https://doi.org/10.1126/science.aam7194

Herman MW, Furlong KP (2016) Revisiting the Canterbury earthquake sequence after the 14 February 2016 M_w 5.7 event. Geophys Res Lett 43:7503–7510. https://doi.org/10.1002/2016GL069528

Holden C, Beavan J (2012) Kinematic source studies of the ongoing (2010–2011) sequence of recent large earthquakes in Canterbury. Paper 061 (8 p). In: Implementing lessons learnt: 2012 Conference, 13–15 April, Christchurch, New Zealand. New Zealand Society for Earthquake Engineering, Christchurch

Holden C, Bannister SC, Beavan RJ, Cousins WJ, Field BJ, McCaffrey R, Reyners ME, Ristau J, Samsonov S, Wallace LM (2008) The M_w 6.6 Gisborne earthquake of 2007: preliminary records and general source characterisation. Bull NZ Soc Earthq Eng 41:266–277

Holden C, Kaiser A, Van Dissen R, Jury R (2013) Sources, ground motion and structural response characteristics in Wellington of the 2013 Cook Strait earthquakes. Bull NZ Soc Earthq Eng 46:188–195

Holt RA, Savage MK, Townend J, Syracuse EM, Thurber CH (2013) Crustal stress and fault strength in the Canterbury Plains, New Zealand. Earth and Planet Sci Lett 383:173–181. https://doi.org/10.1016/j.epsl.2013.09.041

Horspool NA, Chadwick MP, Ristau J, Salichon J, Gerstenberger MC (2015) ShakeMapNZ: informing post-event decision making. Paper no. O-40. In: New dimensions in earthquake resilience: 2015 New Zealand Society for Earthquake Engineering technical conference and AGM, 10–12 Apr 2015, Energy Events Centre, Rotorua. New Zealand Society for Earthquake Engineering

Jost ML, Herrmann R (1989) A student's guide to and review of moment tensors. Seismol Res Lett 60:37–57

Kaiser A, Holden C, Beavan J, Beetham D, Benites R, Celentano A, Collet D, Cousins J, Cubrinovski M, Dellow G, Denys P, Fielding E, Fry B, Gerstenberger M, Langridge R, Massey C, Motagh M, Pondard N, McVerry G, Ristau J, Stirling M, Thomas J, Uma SR, Zhao J (2012) The M_w 6.2 Christchurch earthquake of February 2011: preliminary report. NZ J Geol Geophys 55:67–90. https://doi.org/10.1080/00288306.2011.641182

Kaiser A, Balfour N, Fry B, Holden C, Litchfield N, Gerstenberger M, D'Anastasio E, Horspool N, McVerry G, Ristau J, Bannister S, Christophersen A, Clark K, Power W, Rhoades D, Massey C, Hamling I, Wallace L, Mountjoy J, Kaneko Y, Benites R, Van Houtte C, Dellow S, Wotherspoon L, Elwood K, Gledhill K (2017) The Kaikoura (New Zealand) earthquake: preliminary seismological report. Seismol Res Lett 88. https://doi.org/10.1785/0220170018

Kao H, Jian P-R, Ma K-F, Huang B-S, Liu C-C (1998) Moment-tensor inversion for offshore earthquakes east of Taiwan and their implications to regional collision. Geophys Res Lett 25:3619–3622

Kao H, Shan S-J, Bent A, Woodgold C, Rogers G, Cassidy JF, Ristau J (2012) Regional centroid-moment-tensor analysis for earthquakes in Canada and adjacent regions: an update. Seismol Res Lett 83:505–515. https://doi.org/10.1785/gssrl.83.3.505

Kubo A, Fukuyama E, Kawai H, Nonomura K (2002) NIED seismic moment tensor catalogue for regional earthquakes around Japan: quality test and application. Tectonophysics 356:23–48

Langridge R, Van Dissen R, Rhoades D, Villamor P, Little T, Litchfield N, Clark K, Clark D (2011) Five thousand years of surface ruptures on the Wellington fault, New Zealand: implications for recurrence and fault segmentation. Bull Seismol Soc Am 101:2088–2107. https://doi.org/10.1785/0120100340

Little TA, Van Dissen R, Rieser U, Smith EGC, Langridge RM (2010) Coseismic strike slip at a point during the last four earthquakes on the Wellington fault near Wellington, New Zealand. J Geophys Res 115:B05403. https://doi.org/10.1029/2009JB006589

Loubet A, Kaneko Y, Tape C (2016) Validation of 3D velocity and attenuation models in the North Island of New Zealand with full-wavefield simulations. Abstract S41A-2739. In: AGU fall meeting, San Francisco, 12–16 Dec 2016: 2016 fall meeting program. American Geophysical Union, USA

Matcham I, Savage MK, Taber JJ, Reyners ME (2006) Earthquake source mechanism analysis for events between 1992 and 1997 using sparse New Zealand broadband data. NZ J Geol Geophys 49:75–89

Pasyanos ME, Dreger DS, Romanowicz B (1996) Towards real-time determination of regional moment tensors. Bull Seismol Soc Am 86:1255–1269

Petersen T, Ristau J, Beavan J, Denys P, Denham M, Field B, Francois-Holden C, McCaffrey R, Palmer N, Reyners M, Samsonov S, The GeoNet team (2009) The M_w 6.7 George Sound earthquake of October 15, 2007: response and preliminary results. Bull NZ Soc Earthq Eng 42:129–141

Petersen T, Gledhill K, Chadwick M, Gale N, Ristau J (2011) The New Zealand seismograph network. Seismol Res Lett 82:9–20. https://doi.org/10.1785/gssrl.82.1.9

Reyners M (1989) New Zealand seismicity 1964–87: an interpretation. NZ J Geol Geophys 32:307–315

Reyners M, McGinty P, Cox S, Turnbull I, O'Neill T, Gledhill K, Hancox G, Beavan J, Matheson D, McVerry G, Cousins J, Zhao J, Cowen H, Caldwell G, Bennie S, The GeoNet team (2003) The M_w 7.2 Fiordland earthquake of August 21, 2003: background and preliminary results. Bull NZ Soc Earthq Eng 36:233–248

Reyners M, Bannister S (2007) Earthquakes triggered by slow slip at the plate interface in the Hikurangi subduction zone, New Zealand. Geophys Res Lett 34:L14305. https://doi.org/10.1029/2007GL030511

Ristau J (2008) Implementation of routine regional moment tensor analysis in New Zealand. Seismol Res Lett 79:400–415. https://doi.org/10.1785/gssrl.79.3.400

Ristau J (2009) Comparison of magnitude estimates for New Zealand earthquakes: moment magnitude, local magnitude, and teleseismic body-wave magnitude. Bull Seismol Soc Am 99:1841–1852. https://doi.org/10.1785/0120080237

Ristau J (2011) Focal mechanism analysis of Christchurch Boxing Day aftershocks. GNS Science Consultancy Report 2011/43, 7 p

Ristau J (2013) Update of regional moment tensor analysis for earthquakes in New Zealand and adjacent offshore regions. Bull Seismol Soc Am 103:2520–2533. https://doi.org/10.1785/0120120339

Ristau J (2017) Source characteristics of the 2016 Kaikoura and Te Araroa, New Zealand, earthquake sequences from regional moment tensor analysis. Seismol Res Lett 87:654. https://doi.org/10.1785/0220170035

Ristau J, Rogers GC, Cassidy JF (2007) Stress in western Canada from regional moment tensor analysis. Can J Earth Sci 44:127–148. https://doi.org/10.1139/E06-057

Ristau J, Holden C, Kaiser A, Williams C, Bannister S, Fry B (2013) The Pegasus Bay aftershock sequence of the M_w 7.1 Darfield (Canterbury), New Zealand earthquake. Geophys J Int 195:444–459. https://doi.org/10.1093/gji/ggt222

Ristau J, Harte D, Salichon J (2016) A revised local magnitude (M_L) scale for New Zealand earthquakes. Bull Seismol Soc Am 106:398–407. https://doi.org/10.1785/0120150293

Robinson R (1986) Seismicity, structure and tectonics of the Wellington region, New Zealand. Geophys J R Astron Soc 87:379–409

Rodgers DW, Little TA (2006) World's largest coseismic strike-slip offset: the 1855 rupture of the Wairarapa fault, New Zealand, and implications for displacement/length scaling of continental earthquakes. J Geophys Res 111(B12408). https://doi.org/10.1029/2005jb004065

Ruppert NA, Hansen RA (2010) Temporal and spatial variations of local magnitudes in Alaska and Aleutians and comparison with body-wave and moment magnitudes. Bull Seismol Soc Am 100:1174–1183. https://doi.org/10.1785/0120090172

Scognamiglio L, Tinti E, Michelini A (2009) Real-time determination of seismic moment tensor for the Italian region. Bull Seismol Soc Am 99:2223–2242. https://doi.org/10.1785/0120080104

Seeback H, Nicol A, Villamor P, Ristau J, Pettinga J (2014) Structure and kinematics of the Taupo rift, New Zealand. Tectonics 33:1178–1199. https://doi.org/10.1002/2014TC003569

Sipkin SA (1986) Estimation of earthquake source parameters by the inversion of waveform data: global seismicity. Bull Seismol Soc Am 76:1515–1541

Stirling M, McVerry G, Gerstenberger M, Litchfield N, Van Dissen R, Berryman K, Barnes P, Wallace L, Villamor P, Langridge R, Lamarche G, Nodder S, Reyners M, Bradley B, Rhoades D, Smith W, Nicol A, Pettinga J, Clark K, Jacobs K (2012) National seismic hazard model for New Zealand: 2010 update. Bull Seismol Soc Am 102:1514–1542. https://doi.org/10.1785/0120110170

Townend J, Sherburn S, Arnold R, Boese C, Woods L (2012) Three-dimensional variations in present-day tectonic stress along the Australia-Pacific plate boundary in New Zealand. Earth Planet Sci Lett 353–354:47–59. https://doi.org/10.1016/j.epsl.2012.08.003

Van Dissen RJ, Berryman KR (1996) Surface rupture earthquakes over the last ~1000 years in the Wellington region, New Zealand, and implications for ground shaking hazard. J Geophys Res 101(B3), 5999–6019

Wallace LM, Cochran UA, Power WL, Clark KJ (2014) Earthquake and tsunami potential of the Hikurangi subduction thrust, New Zealand: insights from paleoseismology, GPS, and tsunami modelling. Oceanography 27:104–117. https://doi.org/10.5670/oceanog.2014.46

Wessel P, Smith WHF (1998) New, improved version of generic mapping tools released, *EOS, Transactions*. Am Geophys Union 79:579

Whidden KM, Pankow KL (2012) A catalog of regional moment tensors in Utah from 1998 to 2011. Seismol Res Lett 83:775–783. https://doi.org/10.1785/0220120046